Proc. of the X Int. Conf. — Ion Implantation and other Applications of Ions and Electrons, Kazimierz Dolny 2014

Temperature Dependent Catalytic Activity of Ag/PET Ion-Track Membranes Composites

D. Borgekov[a,b], A. Mashentseva[a,b*], S. Kislitsin[a], A. Kozlovskiy[a,b], A. Russakova[b] and M. Zdorovets[a,b]

[a]Institute of Nuclear Physics, Ibrahimov str., 1, 050032, Almaty, Kazakhstan

[b]The L.N. Gumilyov Eurasian National University, Satpaev str., 2, 010008 Astana, Kazakhstan

Electroless deposition has been used to coat finely porous polyethylene terephthalate (PET) track-etched membranes with silver, forming silver nanotubes within the pores with inner and outer diameters of 60 and 100 nm. The sample's X-ray diffraction pattern shows a face-centered cubic crystalline phase of silver with the lattice constant 4.0838 nm. The average size of silver nanoclusters, as obtained from the scanning electron microscopy analysis is about 30 nm which is consistent with the X-ray diffraction results. The temperature dependent catalytic activity of prepared composites is demonstrated for two model reactions such as reduction of 4-nitrophenol (4-NP) and decomposition of hydrogen peroxide. Apparent constant rates and activation energy as well as reusability of catalysts were determined. The developed composite catalyst could be used consecutively for several runs without any damages for 4-NP reduction. For hydrogen peroxide reaction decomposition the reaction rate of the second cycle is reduced 2.4 times. Moreover, the second reuse reduced conversion of H_2O_2 to 54.7% suggests removal of active Ag centers during the first cycle of testing.

DOI: 10.12693/APhysPolA.128.871

PACS: 62.23.Pq, 82.65.+r, 82.20.Pm

1. Introduction

Due to their unique properties such as possibility to control shape and size of pores, flexibility and high chemical resistance track-etched membranes (TeMS) are widely used as a support template for electroless or electrochemical deposition of various materials [1]. After dissolving of the polymer matrix in an appropriate solvent, the resulting highly ordered arrays of nanotubes (NTs) or nanowires (NWs) find extensive application in various fields of material science, including electrochemical sensing [2] and biosensing [3], nanoelectronics [4] and magnetic materials [5], medicine and biotechnology [6, 7]. "As-prepared" TeMs with the embedded metal nanoparticles/NTs also could be applied as highly efficient heterogeneous catalysts for the reactions which occurred on both the membrane surface and through them [8]. One of the main advantages of TeMs-based composites as a catalyst is a membrane geometry that allows to distribute uniformly the catalytically active material over the entire surface of the pores and carried out reactions without separation of nanosized catalysts from the reaction mixture after the reaction is completed. The polymer template could be also easily removed and cleaned without contaminating and morphologically changing the formed nanostructures [9]. Recently there have been several reports that demonstrated the catalytic activity of metallic NTs embedded in porous TeMs: thus, the reduction of 4-NP as a benchmark model reaction was studied for the Au/PET and Au/Ag/PET composites [10], flow-through experiments were performed for silver and gold [11], Ag–Pt [12], NTs membranes in polycarbonate (PC) TeMs. The unsupported Pt NWs showed better catalytic activity for methanol oxidation than those supported in the PC template [9], also Au NTs, loaded in the same template was used as a membrane reactor for CO oxidation [13].

However, most of the previous studies focused on the improvement of synthesis strategy [14] or on simple testing of catalytic activity in different model systems, therefore the temperature dependent activity ion-track membranes composites have not been studied yet.

In this paper, the fabrication of silver NTs of about 100 ± 5 nm in diameter and 12 μm long as well as elucidation of their composition and structure were discussed. Temperature dependent catalytic properties of the prepared Ag/PET composite membranes were tested for reduction of 4-NP to 4-AP and at the first time as catalysts for decomposition of hydrogen peroxide in the aqueous media.

2. Experiment

2.1. Template preparation

The PET film (Hostaphan® RNK, Mitsubishi Polyester Film, nominal thickness of 12 μm) was irradiated with 1.75 MeV/nucl Kr-ion beam with the ion fluency of 1×10^9 cm^{-2} at the DC-60 cyclotron in Astana and etched in the 2.2 M sodium hydroxide solution at 85 °C for 75 s that provides formation of 100 ± 5 nm cylindrical pores. The effective pore sizes of parent template as well as the inner diameter of NTs were estimated by gas permeability using the equation

*corresponding author; e-mail: mashentseva.a@gmail.com

$$Q = \frac{4\pi r^3}{3l}\sqrt{\frac{2\pi}{RTM}}\Delta p, \quad (1)$$

where Q is the molar flow rate of air through the pore, R is the gas constant, M is the molecular weight, L is the membrane thickness, Δp is the applied pressure.

2.2. Electroless plating

The improved electroless deposition technique reported by Muench [11] was used. Prior to electroless plating the PET membrane was immersed into a solution of $SnCl_2$ (25 g/L) and hydrochloric acid (60 g/L) for 15 min to sensitize polymer surface and thoroughly rinsed for 15 min under flowing water. Afterward the activated templates were deposited in the aqueous plating solutions containing $AgNO_3$ (17 mM), potassium sodium tartrate (120 mM) and pyridine (50 mM) as a complexing agent. Deposition took place at 2–4 °C, after the desired deposition time (1 h) Ag-plated composite membranes were washed in water and ethanol and dried in air.

2.3. Characterisation

Scanning electron microscopy (SEM) and energy-dispersive X-ray spectroscopy (EDAX) were performed using a JEOL-7500F (JEOL, Japan) equipped with iXRF EDS -2000 (Oxford Instruments). Prior to the measurement, the PET template was removed with 1,1,1,3,3,3-hexafluoro-2-propanol and template-free Ag NTs were collected on the carbon tape and sputter-coated with gold.

The X-ray diffraction (XRD) pattern was obtained on a D8 Advance (Bruker, Germany) to study the crystalline structure of the sample with a fixed anode Cu source. X-ray was generated at 40 mA and 40 kV, and the scanning position ranged from 20−150°2(θ). The crystal silver grain size was calculated from the diffractogram peak shape using the Scherrer equation

$$\tau = \frac{k\lambda}{\beta\cos\theta}, \quad (2)$$

where the shape factor $k = 0.9$, λ is 1.54 Å, β — the full width half maximum (FWHM) and θ — the Bragg angle.

2.4. Catalysis

The catalytic activity of "as-prepared" Ag/PET membranes was determined by reduction of 4-NP to 4-AP by $NaBH_4$ according to the experimental procedure described in [15]. Afterwards the sample of Ag/PET composites (size about 5×5 cm^2) was immersed in a beaker and catalytic activity was monitored by every 5 min absorbance measurements using the Specord-250 spectrophotometer (Jena Analytic, Germany) recording the absorption spectra in the range 200–600 nm. After the reaction, the Ag/PET membrane was thoroughly rinsed with deionized water and used in the next 4 cycles without any additional pretreatment.

The catalytic decomposition of H_2O_2 was made in a 250 mL round-bottomed flask immersed in a water bath at 25–45 °C. For each test, 5.75×4.25 cm^2 of the Ag/PET catalyst was used. The reaction time was recorded after the addition of 50 mL (1.02 wt% H_2O_2) solution preheated at the same operating temperature. The standard H_2O_2 solution was prepared by dilution and its concentration was standardized by a potassium dichromate solution. A graduated glass burette was used to measure the O_2 volume. After complete decomposition of H_2O_2, the catalysts were thoroughly rinsed with deionized water.

3. Discussion

XRD analysis was used to characterize chemical composition and crystal structure of the silver NTs array. The typical XRD pattern and corresponding intensity of the major peaks of Ag NTs are shown in Fig. 1a.

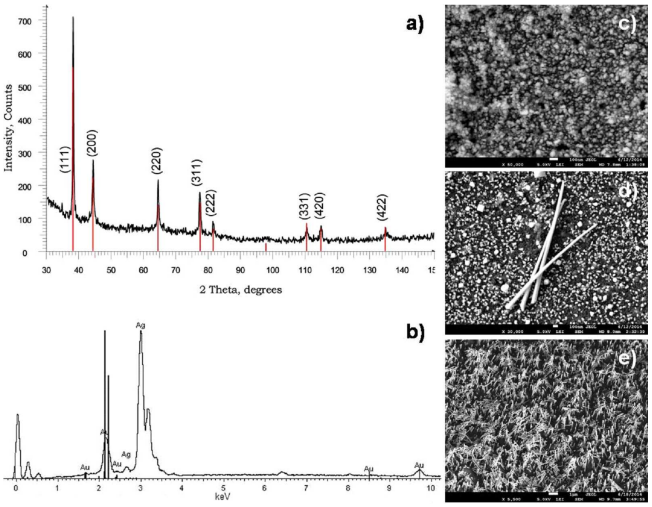

Fig. 1. (a) XRD pattern of Ag nanotubes separated from a PET template. The bottom red vertical lines show the peak positions and relative intensities of pure powder Ag (JCPDS 4-0783). (b) EDX spectra of Ag NTs after removal of the polymer template. (c–d) SEM images of composites surface and (e) Ag NTS arrays without the template.

As follows from the XRD spectra, the isolated Ag NTs exhibited diffraction peaks at 2θ values: 38.16°, 44.35°, 64.53°, 77.48°, 81.55°, 110.58° and 115.01° corresponding to (111), (200), (220), (311), (222), (331), and (420) planes of silver, respectively [16]. Thus the XRD spectrum confirmed the crystalline structure of silver NTs. All the peaks in the XRD pattern can be readily indexed to a face-centered cubic structure of silver as reported in the available literature (JCPDS 4-0783). The lattice constant calculated from this pattern was found to be $a = 4.0838 \pm 0.035$ nm, which is consistent with the standard value $a = 0.4086$ nm. The average crystallite size was estimated from the diffracting planes along the direction normal to the (hkl) plane applying the Scherrer formula (2) and was 24.57 ± 4 nm.

The elemental analysis of sample has been performed using the EDX spectroscopy. Figure 1b shows the EDX

spectrum of template-free silver NTs. The peaks observed at 3.0, 3.2, and 3.4 keV correspond to the binding energies of Ag L_α, Ag L_β, and Ag $L_{\beta 2}$, respectively. The gold peaks correspond to the gold sputtered on sample holder before the SEM analysis. The obtained nanostructures have a tubular morphology and are uniform in terms of their length (12 μm). The effective thickness of silver nanotube walls was determined with Eq. (1) to be about 40 ± 4.2 nm.

Figure 1c–e depicts the SEM images of the surface Ag/PET composite membranes and free standing Ag NTs. As it was determined from Fig. 1c, the average size of Ag nanoclusters on the surface is $\approx 30 \pm 3$ nm, which is consistent with the XRD results.

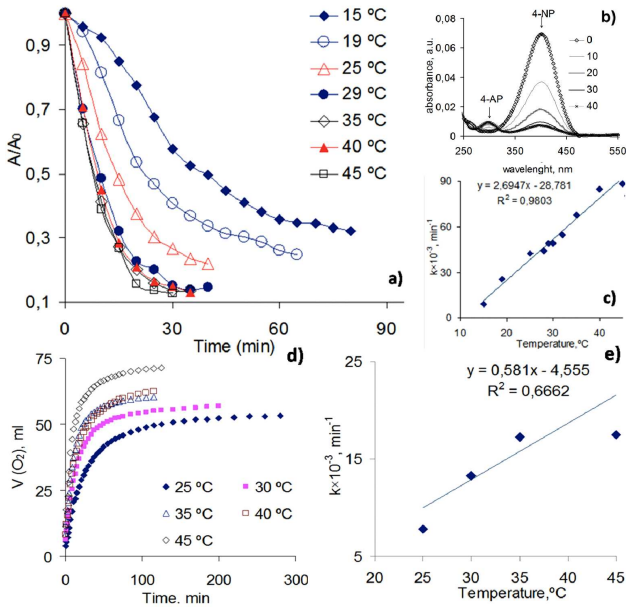

Fig. 2. (a) Effect of reaction temperature on the reduction of 4-NP over Ag/PET composite. (b) UV-Vis spectra of the studied model reaction under the running temperature of 35 °C and (c) correlation of apparent rate constant and reaction temperature. (d) Catalytic decomposition of H_2O_2 over the Ag/PET composite: evolving of oxygen as a function of time. (e) Variation of rate constant values at reaction temperatures.

In order to investigate the effect of temperature on the reduction of 4-NP in the aqueos solution catalyzed by PET/Ag membrane composites, the experiments with different temperatures (15–45 °C) were set up. Figure 2a shows that 4-NP reduction efficiencies increased gradually with the temperature rise from 15 to 45 °C. It was also observed that at lower temperatures, the required time was very long. A typical UV–V is absorption change of a solution containing 4-NP and $NaBH_4$ is shown in Fig. 2b. Because the reaction is the pseudo-first order in the presence of excess of reducing agent ($NaBH_4$) [17], the apparent rate constant (min^{-1}) was calculated from the slope of a plot of the natural log of the absorbance at 400 nm yields (A/A_0). Figure 2c shows that k_{app} increased rapidly from 0.0093 to 0.0866 min^{-1} when the temperature increased from 15 to 45 °C. The 4-NP conversion degree was increased from 66.1% (15 °C) to 88.6% (45 °C). By testing the catalytic activity at different temperatures the apparent activation energy (E_A) was calculated via the Arrhenius plot of the $k_{app} = f(1/T)$ and it was found to be $E_A = 51.19$ kJ mol^{-1}.

Although direct comparison with similar results, published in other reports dealing with silver as a nanosized catalyst for reduction of 4-NP is difficult due to inconsistent reaction conditions such as concentration of initial chemicals, type and size of silver catalyst (i.e. nanoparticles, NWs, NTs, temperature). Thus, for silver nanoparticles with diameter of 7–15 nm [17] an activation energy was found to be $E_A = 41$ kJ mol^{-1}, while for Ag supported nanoclusters $E_A = 55.6$ kJ mol^{-1} [18], for 10 nm silver nanoparticles deposited on polyaniline bridged silica networks the activation energy was claimed to be $E_A = 192$ kJ mol^{-1} [19].

Also Ag/PET membrane composites were tested for H_2O_2 decomposition. Hydrogen peroxide is a versatile oxidizing reagent thanks to its excellent properties including safety, high efficiency, and low pollution [20]. It could be applied for water pollutant decomposition and for green oxidation processes [21]. The kinetics of the catalytic decomposition of hydrogen peroxide was conducted at 25, 30, 35, 40 and 45 °C. The analysis of the experimental data was made on the assumption that decomposition of H_2O_2 is the first order process. The volume of the evolved oxygen was plotted as a function of time (Fig. 2d). From the slope of the straight lines, the apparent rate constants k were obtained. The dependence of apparent constant rate on temperature is shown in Fig. 2e. The apparent activation energy (E_A) was evaluated as described below and was $E_A = 34.35$ kJ mol^{-1}.

TABLE

Reusability of the Ag/PET catalyst in the studied reactions.

Cycle	Apparent constant rate $[k \times 10^{-3}$ $min^{-1}]$		Conversion of initial reagent	
	4-NP→4-AP	H_2O_2 decomp.	4-NP→4-AP	H_2O_2 decomp.
fresh run	85.0	16.5	89.8%	73.53%
2nd run	69.3	7.0	87.1%	54.7%
3rd run	66.5	–	80.3%	–

The reusability of the catalyst is an important factor from the economical and environmental points of views and has attracted much attention in recent years. The reusability of the prepared Ag/PET composites was examined three times at 40 °C for both studied reactions. As shown in the Table in the case of applying Ag/PET composite membranes for reduction of 4-NP, the constant rate slowly decreases, the composite surface does not damage during this reaction [22]. For decomposition of hydrogen peroxide reaction, the reaction rate of

the second cycle is decreased 2.4 times as well as second reuse reduce conversion of H_2O_2 to 54.7% suggesting removal of active Ag with the smallest diameter from the surface of the composite membrane since reaction is carried out under vigorous release of oxygen during the first cycle of testing. In order to confirm Ag nanoparticles removal and aggregation after first run, the XRD analysis was carried out immediately after 1st cycle of testing in H_2O_2 decomposition reaction was done. As it was determined from the Scherrer equation, Ag crystallite sizes were slightly increased, thus after first run testing at 40 °C, $d = 14.54$ nm, after second run diameter of crystallites was increased up to 18.52 nm.

Thus, excellent reusability of the catalytic activity for the studied composites was observed only for the reaction of the reduction of *p*-nitrophenol. Decomposition reaction of hydrogen peroxide under Ag/PET composite membrane probably requires additional binding of silver nanoparticles with the membrane's surface.

4. Conclusions

In this paper structurally well-defined silver NTs with the inner and outer diameters of 60 and 100 nm and length of *ca.* 12 μm were prepared via the polymer template-synthesis method by electroless deposition of silver within the pores of a track-etched PET membrane. The catalyst stability in reduction of 4-NP has also been demonstrated convincingly by conducting three successive runs without a significant drop in the reaction rate. For hydrogen peroxide reaction decomposition, the reaction rate of the second cycle at 40 °C decreased 2.4 times due to removal of active Ag centers during the first cycle of testing. Further extension of the Ag/PET composites catalytic system to another key application is currently being explored.

Acknowledgments

The authors would like to thank Dr. Anastassiya Migunova (INP) for her help with XRD measurements.

References

[1] S. Demoustier-Champagne, M. Delvaux, *Mater. Sci. Eng. C* **15**, 269 (2001).

[2] E.-M. Felix, F. Muench, W. Ensinger, *RSC Adv.* **4**, 24504 (2014).

[3] M. Garcia, P. Batalla, A. Escarpa, *TrAC* **57**, 6 (2014).

[4] A. Moncada, M.C. Mistretta, S. Randazzo, S. Piazza, C. Sunseri, R. Inguanta, *J. Power Sources* **256**, 72 (2014).

[5] M.-C. Clochard, M. El Jouad, N. Biziere, Pham Do Chung, H.-J. Drouhin, E. Balanzat, D. Lairez, M. Viret, J.-E. Wegrowe, *Rad. Phys. Chem.* **94**, 66 (2014).

[6] V. Rao, J.V. Amar, D.K. Avasthi, R. Narayana Charyulu, *Radiat. Meas.* **36**, 585 (2003).

[7] M.Y. Kim, D.J. Li, L.K. Pham, B.G. Wong, E.E. Hui, *J. Membrane Sci.* **452**, 460 (2014).

[8] F. Muench, M. Oezaslan, M. Rauber, S. Kaserer, A. Fuchs, E. Mankel, J. Brötz, P. Strasser, C. Roth, W. Ensinger, *J. Power Sources* **222**, 243 (2013).

[9] S.M. Choi, J.H. Kim, J.Y. Jung, E.Y. Yoon, W.B. Kim, *Electrochim. Acta* **53**, 5804 (2008).

[10] A. Mashentseva, D. Borgekov, M. Zdorovets, A. Russakova, *Acta Phys. Pol. A* **125**, 1263 (2014).

[11] F. Muench, M. Rauber, C. Stegmann, S. Lauterbach, U. Kunz, H.-J. Kleebe, W. Ensinger, *Nanotechnology* **22**, 415602 (2011).

[12] F. Muench, S. Lauterbach, H.-J. Kleebe, W. Ensinger, *e-J. Surf. Sci. Nanotechnol.* **10**, 578 (2012).

[13] M.A. Sanchez-Castillo, C. Couto, W.B. Kim, J.A. Dumesic, *Angew. Chem. Int. Ed.* **43**, 1140 (2004).

[14] F. Muench, S. Bohn, M. Rauber, T. Seidl, A. Radetinac, U. Kunz, S. Lauterbach, H-J. Kleebe, C. Trautmann, W. Ensinger, *J. Appl. Phys. A* **116**, 287 (2014).

[15] Y. Yu, K. Kant, J.G. Shapter, *Microporous Mesoporous Mater.* **153**, 131 (2012).

[16] M.A.M. Khan, S. Kumar, M. Ahamed, S.A. Alrokayan, M.S. AlSalhi, *Nanoscale Res. Lett.* **6**, 434 (2011).

[17] N. Pradhan, A. Pal, T. Pal, *Coll. Surf. A* **196**, 247 (2002).

[18] A. Leelavathi, T.U.B. Rao, T. Pradeep, *Nanoscale Res. Lett.* **6**, 123 (2011).

[19] K.M. Manesh, A.I. Gopalan, K.-P. Lee, S. Komathi, *Catal. Commun.* **11**, 193 (2010).

[20] I. Korolkov, A. Mashentseva, D. Niyazova, O. Güven, M. Barsbay, M. Zdorovets, *Polym. Degr. Stab.* **107**, 150 (2014).

[21] T. Kiyonaga, Q. Jin, H. Kobayashi, H. Tada, *Chem. Phys. Chem.* **10**, 2935 (2009).

[22] A. Mashentseva, D. Borgekov, S. Kislitsin, M. Zdorovets, A. Migunova, *Nucl. Instrum. Methods Phys. Res. B* **365**, 70 (2015).